

# Torque Control for a Form Tool Drilling Operation

Richard J. Furness, Tsu-Chin Tsao, *Member, IEEE*, James S. Rankin, II, Michael J. Muth, and Kenneth W. Manes

**Abstract**—Torque control through feed manipulation can provide significant machining economic benefit for drilling processes by preventing tool breakage and reducing cycle time. This paper presents the dynamic modeling and real-time torque control for a form tool drilling process. The form tool produces a desired shape in a workpiece through a drilling process. In this study, the form tool drilling process resembles the combination of drilling, reaming, counter-boring, and chamfering operations. The machining process is modeled as a linear system with variable gain due to the form tool geometry. The process is also subject to unknown disturbances such as unpredictable chip jamming and tool-workpiece friction. Spindle motor power and speed measurements were used to estimate drilling torque for cost effective practical implementation. An input-output pole placement controller with previewed gain scheduling was designed and implemented. Through experimental studies, this controller was shown to effectively regulate tool torque and hence avoid tool breakage, by manipulating the feed during drilling, and reduce cycle time compared to current practice.

**Index Terms**—Drilling, load prediction, manufacturing, pole placement design, process control.

## I. INTRODUCTION

**D**RILLING REMAINS ONE of the most common machining operations, and has been reported to account for up to 50% of all machining nationwide. In spite of such dramatic statistics, drilling has failed to receive significant attention with respect to the numerous potential benefits of process control. These benefits can include cycle time, tool breakage, and cost reductions, in addition to part quality improvements. Drilling is often viewed as a roughing operation, which is followed by secondary operations to produce desired part attributes (e.g., reaming, deburring, tapping). However, drilling has a direct impact on final quality, and inherently affects the production rate and cost of all following operations. Thus, improvements in drilling process performance can have significant ramifications with respect to overall quality, productivity, and cost.

Tool breakage and cycle time are important concerns for any drilling operation. Breakage interrupts production, leads to scrap and/or rework costs, and if not quickly detected, may lead to catastrophic failures in subsequent processing operations. During drilling, disturbance loads due to factors such as chip jamming, friction, and tool wear can be quite significant, and may lead to catastrophic tool breakage. In practice, the cutting conditions (i.e., feed rate and spindle

speed) are constant during the machining cycle. Conservative cutting conditions are often utilized for drilling operations due to the pervasive uncertainty of the process and the lack of monitoring and control technology. Real-time drilling process control, whereby the machining loads are regulated by manipulating the cutting conditions, presents an opportunity to reduce cycle time and avoid tool breakage. In addition to the improvements for the particular drilling operation, the benefits of process control can extend to subsequent part processing operations.

The cost of machining, tooling, part transferring, and fixturing has driven the trend toward combining several machining operations into one through the use of a form tool to generate a particular geometry. In this study, drilling, reaming, counter-boring, and chamfering operations are performed on a single form tool with variable geometry along its body length. Although there may be significant benefits with respect to total machining cost using such tools, there are typically greater demands on process performance with respect to tool breakage and cycle time. For form tool drilling operations, breakage is a particular concern since the tools are quite expensive, and production is interrupted with no intermediate buffer available. Real-time control and/or monitoring requires precise modeling of the process, but is complicated by the fact that the tool geometry, and hence, the dynamic process model, is continuously variable along its body length.

## II. PROBLEM DESCRIPTION

This study was motivated by a form tool breakage problem for an automotive production application. The form tool is a solid carbide, titanium nitride coated tool with a profile that corresponds to the desired part geometry. Under constant feed ( $f$  [in/rev]) and speed ( $N$  [r/min]) machining, excessive cutting loads often lead to tool breakage. For this operation, tool breakage is a significant concern since the tool cost is quite high ( $\approx \$100$ ), and the current operation is a process bottleneck. The form tool is also intended to be reground several times, raising the significance of catastrophic tool breakage.

### A. Process Description

The form tool geometry, as shown in Fig. 1, consists of three primary sections. The first section is the tapered end of the tool (A), followed by a constant diameter section (B), and a combined counter-bore and chamfer section (C). The drilling process involves three primary machining phases (phases A, B, and C) as these tool sections enter the workpiece. A constant spindle speed and feed are used throughout the production machining operation. In this real-time process

Manuscript received March 17, 1996; revised April 7, 1998. Recommended by Associate Editor, G. C. Verghese.

R. J. Furness, J. S. Rankin, II, and M. J. Muth are with Ford Research Laboratories, Ford Motor Company, Detroit, MI, 48202 USA.

T.-C. Tsao is with the Department of Mechanical and Industrial Engineering, University of Illinois at Urbana-Champaign, Urbana, IL 61801 USA.

K. Manes is with Ford Motor Company, Detroit, MI 48202 USA.

Publisher Item Identifier S 1063-6536(99)00615-6.

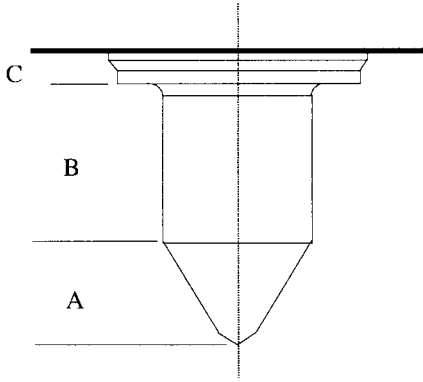


Fig. 1. Form tool geometry.

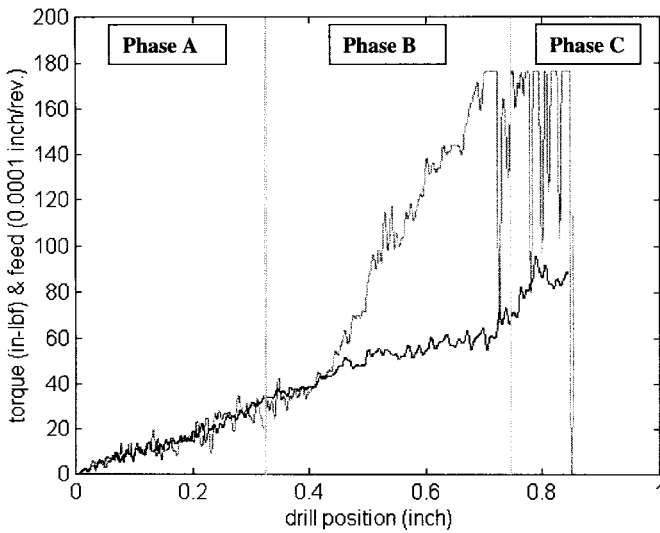


Fig. 2. Measured drilling torque signals from two consecutive tests with identical constant feed cutting conditions.

control application, the machining feed is manipulated to regulate the total tool torque.

### B. Machining Torque

From a process control perspective, the total torque applied to the tool,  $T_{\text{tool}}$ , during drilling consists of two parts

$$T_{\text{tool}} = T_{\text{cut}} + T_d. \quad (1)$$

$T_{\text{cut}}$  represents the drilling torque between the drill cutting edges and the workpiece, and  $T_d$  is a disturbance torque.  $T_{\text{cut}}$  is assumed to be a function of controllable cutting conditions, namely the feed,  $f$ , and to a much lesser extent, the spindle speed,  $N$ .  $T_d$  includes contributions from factors such as the friction torque between the tool and the workpiece, and the congestion torque between the tool and the chip.  $T_d$  is dependent not only on cutting conditions but also other uncontrollable factors such as coolant application, chip length/chip motion, and other process disturbances.

As the form tool enters the workpiece, the edges that take part in cutting vary. Consequently, under constant feed, the drilling torque  $T_{\text{cut}}$  varies. The heavy line in Fig. 2 shows the  $T_{\text{tool}}$  profile with a constant feed ( $f = 0.002$  ipr) and spindle

speed ( $N = 2350$  r/min) when no significant disturbance torque exists. The substantial torque increase at the beginning of phase C, where the tool diameter drastically increases, may cause tool breakage. Consequently, a conservative constant feed is used throughout the operation. The measured torque sequence resembles the tool profile as a function of penetration depth. Comparing the tool geometry in the different machining phases to the torque data in Fig. 2, it appears that constant tool torque could be achieved by scheduling an appropriate open-loop feed profile in a CNC part program. This program would prescribe feed commands in a predetermined manner corresponding to the variation in tool geometry compensating for the varying depth-of-cut. Similar strategies have been used in other machining processes, such as turning and milling, where the depth of cut may vary during the process, and the feed is appropriately scheduled in a part program. With respect to the total tool torque expressed in (1), it is important to note that this strategy will only effectively regulate  $T_{\text{cut}}$ , and does not account for the disturbance torque. In milling and turning, this approach can be effective, since disturbance cutting loads can often be neglected.

An important characteristic unique to drilling is the existence of a significant, unpredictable disturbance torque,  $T_d$ . Due to this disturbance load, tool breakage can still occur even when conservative, constant cutting conditions are used. The light line in Fig. 2 illustrates experimental results from a test when excessive torque caused tool breakage at the end of the machining operation. Based on this, it is unlikely that a predetermined feed trajectory in a CNC part program would effectively regulate drilling torque. Fig. 2 shows data from consecutive tests conducted with the same tool, workpiece material, and cutting conditions. These results dramatically illustrate the magnitude and effect of unpredictable process disturbances on the drilling torque, and demonstrate the necessity for real-time closed torque control for the form tool machining operation.

To address the problem of tool breakage due to excessive torque during machining, a closed-loop control system was designed and implemented. This controller effectively tracks specified torque references, and hence, avoids catastrophic tool breakage. In addition, this controller can reduce the machining time compared to current practice, depending on the chosen torque reference.

A brief review of related research in machining process control is given below. This is followed by a description of the experimental system, and a discussion of the process modeling and control design for the form tool application. Experimental results are then presented which demonstrate the effectiveness of closed-loop torque control.

## III. BACKGROUND

Closed-loop control of cutting forces has been extensively studied for many machining operations [1]–[3]. Application of closed-loop control of cutting forces by manipulating the cutting conditions (feed, speed, or depth-of-cut) for machining has generally been referred to as “adaptive” control. Most of the systems have simply been fixed gain (i.e., nonadapt-

tive) controllers, while certain applications have been truly adaptive (i.e., variable-gain) control systems. The majority of the research work has focused on turning and milling operations. Representative efforts for turning are described in [4]–[9]. Force control for milling has been examined in [10]–[12], among others. As shown in many of these previous studies, the force “disturbances” are primarily attributed to variations in the actual cutting load which occur as the tool encounters variable cutting depths or workpiece material properties. However, these types of disturbances are rarely unknown, and the cutting conditions can be calculated off-line based on *a priori* knowledge of the workpiece geometry, material, and tool path. In such a case, feedforward calculation of cutting conditions should be sufficient to maintain constant cutting loads, and a closed-loop/adaptive control approach would not be necessary or justified. In contrast to milling and turning, drilling requires closed-loop control due to the existence of unpredictable process disturbances other than variations in the actual cutting load. These include chip flow blocking and jamming, drill body-workpiece friction and rubbing, and coolant lubrication variations within a drilling cycle. Closed-loop control has been demonstrated to provide significant machining economic benefit for conventional twist drilling processes [13]–[16]. The form tool drilling process control problem addressed in this paper differs from previous drilling process control studies since the process model varies during the machining operation.

#### IV. EXPERIMENTAL SYSTEM AND INSTRUMENTATION

The drilling experimental setup as shown in Fig. 3 consists of a drilling unit mounted on the cross-slide of a computer numerical control (CNC) lathe, sensors, and real-time data acquisition and control computer. The positioning system of the lathe provides the motion control for the drilling operation: the  $z$ -axis drive provides the feed motion, while the  $x$ -axis indexes the drilling unit relative to a stationary workpiece. The CNC lathe provides closed-loop feedrate control. The drilling unit consists of a five horsepower, induction type motor controlled by an adjustable speed drive (ASD).

A laboratory computer was interfaced to the experimental system for data acquisition and control. Using the feedrate override feature of the lathe controller, the programmed feedrate could be varied between zero and 120% of its programmed value through an analog voltage override command. The spindle speed was similarly prescribed by an analog voltage command to the ASD. Note that the ASD does not provide closed-loop spindle speed regulation.

With this drilling setup, the form tool shown in Fig. 1 was used to drill holes in AISI 1020 hot rolled steel workpieces with a hardness of  $HB = 150$ . The workpieces were mounted on a Kistler Type 9293 dynamometer. During all experiments, the feedrate, thrust force, torque, spindle motor power, and spindle speed signals were measured by the control computer.

#### V. PROCESS MODELING

A block diagram of the drilling system dynamics is shown in Fig. 4. Empirical dynamic models of the machine tool

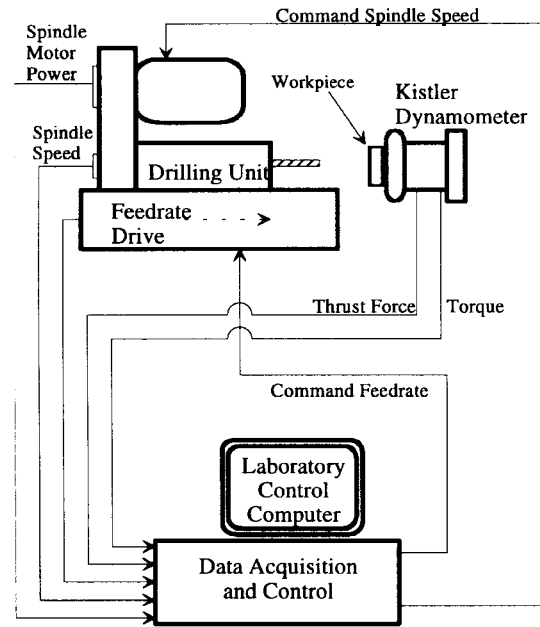


Fig. 3. Experimental system.

drive system, cutting process, and torque sensing system were developed and used for subsequent torque controller design. The command input to the drive system is  $f_{ref}$ . The input to the cutting process is the actual feed,  $f$ , and the output is the cutting torque,  $T_{cut}$ . The torque sensing element provides an estimate ( $T_p$ ) of the actual total tool torque which is used for feedback control. Development of the continuous-time transfer function models is described in the following sections.

##### A. Drive System, $G_f(s)$

The feedrate,  $V$  [inches per minute (in/min)], is the product of the machining feed and the spindle speed,  $N(V = fN)$ . The quantity of interest for torque control is the machining feed, since the chip area (and thus, the chip load) is a function of feed [17]. As denoted by the block diagram above, the dynamic model relating command to actual feed was treated as equivalent to the model between command and actual feedrate. (Note: machine tool drive systems control feedrate not feed. Under constant spindle speed, the two quantities have identical dynamics.) As shown in Fig. 4, a first-order, continuous-time model with delay was considered as the candidate model structure relating command feed. Experimental data was used to estimate the model parameters using least squares identification techniques as

$$\tau_f = 0.058 \text{ s}, \quad L_f = 0.033 \text{ s}. \quad (2)$$

##### B. Cutting Process

The cutting process, relating actual feed to cutting torque, is modeled as a dynamic block that relates feed to chip thickness,  $d$ , cascaded with the cutting process gain ( $K_c$ ) relating chip thickness to the cutting torque

$$G_c(s) = \frac{T_{cut}(s)}{f(s)} = \frac{T_{cut}(s)}{d(s)} \frac{d(s)}{f(s)} = K_c \frac{d(s)}{f(s)}. \quad (3)$$

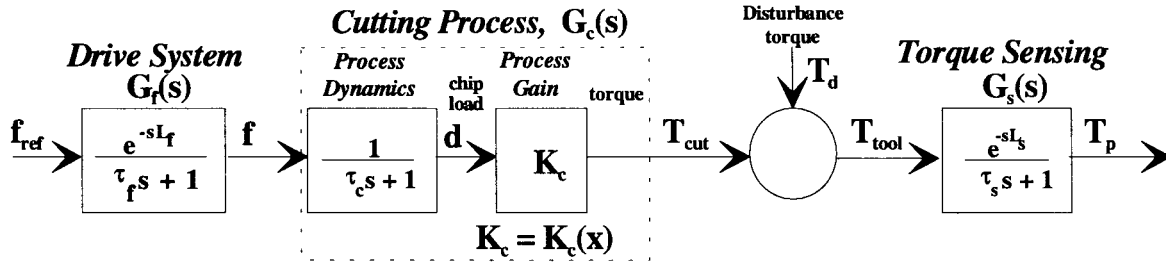


Fig. 4. Drilling system block diagram.

Geometrically, the chip thickness is related to the feed in terms of spindle angle,  $\theta$  [17]

$$\frac{dd}{d\theta} = f(\theta) - f(\theta - \pi) \quad (4)$$

and in the time domain as

$$\frac{dd}{dt} = f(t) - f(t - t_c) \quad (5)$$

where  $t_c = 60/N$  is the rotational period of the two-fluted tool. Based on a first-order Padé approximation of the delay term in the Laplace domain, a first-order transfer function model is commonly used to describe machining process dynamics. Thus, the dynamic model relating chip thickness to feed is

$$\frac{d(s)}{f(s)} = \frac{1}{\frac{t_c}{2}s + 1}. \quad (6)$$

Previous studies have shown that this is an adequate approximation that correlates with empirical first-order drilling process models developed from experimental data [15].

**Open-Loop Gain Estimation:** The data in Fig. 2 clearly show that the cutting process gain,  $K_c$ , varies along the drill body length. For control system design, the process gain is assumed to be piece-wise constant with a step change between machining phases B and C (see Fig. 1). The process gain variation in phase A is not considered here since closed-loop torque control was only implemented during phase B and C. (Note that drilling in phase A does not encounter significant disturbances.) To estimate the drilling process gain, the tool torque was measured by a piezoelectric dynamometer when drilling at three constant feed levels. ( $f_{\text{ref}} = 0.0017, 0.0021, 0.0024$  ipr.) In phases B and C, the average torque was computed, then divided by the feed to estimate the process gain. From these tests, the process gain was estimated to be

$$K_c \left( \frac{\text{in-lb}}{\text{in./rev.}} \right) = 28,000 \text{ for phase B} \\ = 40,000 \text{ for phase C.} \quad (7)$$

These values were used to design and implement a variable gain, closed-loop torque controller. It should be noticed that the gains change with respect to tool wears and workpiece material variations; therefore, a gain margin of 2.0 was specified based on this consideration.

### C. Sensor Modeling—Torque Measurement and Prediction

The actual total tool torque was measured using the piezo-electric dynamometer (see Fig. 3). The instrumentation has saturation limit at about 175 in/lb. For feedback control, a prediction of the actual tool torque,  $T_p$ , was used. The actual torque was estimated using two indirect sensing methods: one based on spindle power sensing and another based on spindle speed measurement. The sensing system dynamics, relating the actual to predicted torque must be included in the control design to ensure stable, robust performance. For the power and spindle speed based methods, the sensor was modeled as a linear first-order continuous-time model with a delay.

**Torque Prediction: Power Measurement Approach:** In this approach, the actual torque was predicted from measurement of spindle motor power. The spindle was belt driven by an AC induction motor. The spindle motor power ( $P$ ) was measured using a power transducer that utilizes Hall Effect sensors.

The tool torque was estimated based on knowledge of the spindle motor electric torque ( $T_e$ ). In general, the static and dynamic behavior of AC induction motors is nonlinear and time-varying. However a linearized transfer function model can be developed about a nominal operating point to give the speed servo loop dynamics [18]. The transfer function relating motor to tool torque can be expressed as

$$\frac{T_e}{T_{\text{tool}}} = \frac{1}{\tau_m s + 1} \quad (8)$$

where  $\tau_m$  is the spindle motor system time constant. The electric torque was calculated from measured power ( $P$ ) and actual spindle speed ( $N_{\text{act}}$ ) as

$$T_e = \frac{\eta P}{N_{\text{act}}} \quad (9)$$

where the coefficient  $\eta$  accounts for the power transducer calibration and drive system efficiency. Utilizing torque data acquired from the dynamometer, the static tool torque prediction based on spindle power was determined to be

$$T_{p,\text{power}} (\text{in/lb}) = 63025 \frac{0.437P (\text{h.p.})}{N_{\text{act}} (\text{r/min.})} \quad (10)$$

The dynamic transfer function model is of the form

$$G_{s,\text{power}}(s) = \frac{T_{p,\text{power}}}{T_{\text{tool}}} = \frac{e^{-sL_s}}{\tau_s s + 1}. \quad (11)$$

With this torque prediction approach, the “sensor” time constant,  $\tau_s$ , is that of the spindle motor system,  $\tau_m$ . The power

transducer signal filtering dynamics were modeled by the pure delay element,  $L_s$ . From measured power and dynamometer torque data, these parameters were estimated to be

$$\tau_s = 0.063 \text{ s}; \quad L_s = 0.033 \text{ s}.$$

This model was incorporated in the overall process transfer function which was utilized to design the closed-loop torque controller. The saturation limit on the power sensor gives predicted torque saturation around 100 in/lb for spindle speed at 2400 r/min.

*Torque Prediction: Spindle Speed-Based Approach:* The second method used to estimate motor electrical torque was based on spindle speed measurement. For induction motors, the steady-state motor electrical torque is a function of the percentage slip [18]. The physical model is a complex nonlinear relationship containing many unknown parameters, some of which vary with speed. For this work, a simplified linear model was used to estimate electrical torque based on spindle speed measurement as

$$T_e = a(N_{\text{ref}} - N_{\text{act}}) \quad (12)$$

where  $N_{\text{ref}}$  is the reference spindle speed. The coefficient  $a$  was estimated from experimental data using the dynamometer torque and spindle speed measurements. The dynamic transfer function relating predicted to tool torque (based on (8)) becomes

$$G_{s,r/\min}(s) = \frac{T_{p,x/\min}}{T_{\text{tool}}} = a(N_{\text{ref}} - N_{\text{act}}) \frac{1}{\tau_s s + 1} \quad (13)$$

where

$$\tau_s = 0.063 \text{ s}.$$

Note that for this spindle speed based torque prediction approach, there is no lag element in the transfer function model. Also note that the time constant is the same for (13) and (11), and corresponds to the spindle drive speed servo loop dynamics.

#### D. Overall Open-Loop Transfer Function

For subsequent controller design, the dynamic models developed in the preceding sections were cascaded to formulate an overall open-loop process transfer function,  $G_p(s)$ , relating command feed to predicted to torque

$$G_p(s) = \frac{T_p(s)}{f_{\text{ref}}(s)} = K_c \frac{e^{-sL_{\text{tot}}}}{(\tau_f s + 1)(\tau_c s + 1)(\tau_s s + 1)} \quad (14)$$

where

$$L_{\text{tot}} = L_f + L_s.$$

## VI. CONTROL SYSTEM DESIGN

The continuous-time open-loop transfer function in (14) was discretized for control design using a sampling rate of 240 Hz. A normalized version of the open-loop transfer function was considered by multiplication of the inverse of the cutting process gain,  $K_c$ , with (14)

$$G'_p(s) = \frac{1}{K_c} \frac{T_p(s)}{f_{\text{ref}}(s)} = \frac{e^{-sL_{\text{tot}}}}{(\tau_f s + 1)(\tau_c s + 1)(\tau_s s + 1)}. \quad (15)$$

By doing this, the plant model for control design is independent of the process gain. A discrete-time control algorithm,  $D(z)$ , was designed using this normalized model, and the controller was subsequently implemented using adaptive gain scheduling. Two control methods were designed and implemented: 1) a proportional-integral (PI) controller and 2) a pole-placement controller. For each design, both power sensor and spindle speed based torque prediction methods were considered. The control objective was to track constant torque references during machining Phases B and C by manipulating the command feed. Since form tool geometry variation could have a significant effect on the cutting process gain,  $K_c$ , it is important that the controller have sufficient gain and phase margins. A gain margin of at least two and a phase margin of  $60^\circ$  were specified design criteria. In addition, the control response must have minimal overshoot. Oscillation in the actual torque due to control system compensation to disturbances is undesirable.

#### A. Previewed Scheduling of Process Gain

The controller was implemented with gain scheduling as a function of tool penetration depth,  $x$  [in]. As mentioned earlier, the transition from drilling phase B to C caused a step change in process gain from 28 000 to 40 000. To avoid a large torque overshoot at the transition, a preview of this step change was incorporated in the gain schedule adaptation strategy to account for the delay between the feed rate command and the actual feed rate. The gain switches at a distance ahead of the phase B and C junction and the value is determined in real-time by multiplying the actual feed rate with the feed drive delay, which is approximated by the pure delay plus the time constant

$$\begin{aligned} \hat{K}_c &= 28\,000 & \text{if } (x^* - x(k)) \geq (L_f + \tau_f)V_{\text{act}}(k) \\ \hat{K}_c &= 40\,000 & \text{if } (x^* - x(k)) < (L_f + \tau_f)V_{\text{act}}(k) \end{aligned} \quad (16)$$

where  $x^*$  is the transition depth from phase B to C ( $x^* = 0.745''$ ).

#### B. Digital P-I Control

PI control was considered first since it is commonly used for fixed set-point regulation. The normalized, continuous-time transfer function model in (15) was discretized using a zero-order hold equivalence transformation for a sampling rate of 240 Hz [19]. The discrete transfer function is

$$G'_p(z) = \frac{1}{K_c} \frac{T_p(z)}{f_{\text{ref}}(z)} = \frac{0.001(0.233z^2 + 0.830z + 0.184)}{z^{16}(z^3 - 2.584z^2 + 2.210z - 0.625)}. \quad (17)$$

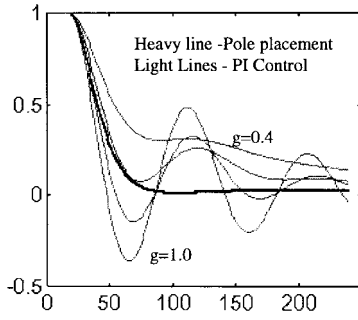


Fig. 5. Simulated closed-loop response to a step disturbance input. (Heavy line: pole placement, light line: PI controls.)

By applying the Ziegler–Nichols transient response method [19], the PI controller was determined to be

$$D_{PI}(z) = g \frac{2.5714z - 0.9467}{z - 1} \quad (g = 1). \quad (18)$$

From both simulation and experimental tests, the P-I design was shown to result in an undesirable oscillatory response. Consequently, a factor  $g$  was introduced to reduce the loop gain to provide a controller response without overshoot. Fig. 5 shows the controller responses to a unit step disturbance for the values of  $g = 1.0, 0.8, 0.6, 0.4$ . A value of  $g = 0.4$ , which gives gain margin of 3.3 and  $97.5^\circ$ s phase margin, was determined to be acceptable with respect to controller overshoot; however, as shown below, the transient response with this design was quite sluggish.

### C. Pole Placement with Integral Action

To improve the transient response performance, a pole placement with integral action controller was considered. To avoid a large controller order resulted from the long overall open-loop process delay in (15), the delay was modeled by a second-order Padé approximation. The approximate, normalized continuous-time open-loop transfer function becomes

$$\begin{aligned} G'_p(s) &= \frac{1}{K_c} \frac{T_p(s)}{f_{ref}(s)} \\ &= \frac{1 - (sL_{tot}/2) + ((sL_{tot})^2/12)}{(1 + (sL_{tot}/2) + ((sL_{tot})^2/12))(\tau_f s + 1)(\tau_c s + 1)(\tau_s s + 1)}. \end{aligned} \quad (19)$$

The discrete transfer function for (28) at a sampling rate of 240 Hz is

$$\begin{aligned} G'_p(z) &= \frac{1}{K_c} \frac{T_p(z)}{f_{ref}(z)} \\ &= \frac{0.001(0.192z^4 + 0.102z^3 - 0.964z^2 + 0.567z + 0.151)}{(z^5 - 4.232z^4 + 7.156z^3 - 6.042z^2 + 2.548z - 0.429)}. \end{aligned} \quad (20)$$

The pole placement controller has the form of

$$R(z)f_{ref}(k) = M(z)T_{ref}(k) - S(z)T_p(k). \quad (21)$$

The polynomials  $R(z)$ ,  $M(z)$ , and  $S(z)$ , are chosen to satisfy desired closed-loop controller performance. To design a

polynomial based pole placement control, a reference model of the desired closed-loop system is utilized. The input–output model without cancellation of any plant zeroes is specified as

$$G_{CL}(z) = \frac{T_p(z)}{T_{ref}(z)} = \frac{B_m(z)}{A_m(z)} \quad (22)$$

where  $B_m$  and  $A_m$  give the desired torque response ( $T_p$ ) to command references ( $T_{ref}$ ). For this application, the discrete-time denominator polynomial is

$$\begin{aligned} A_m(z) &= z^5 - 4.242z^4 + 7.190z^3 - 6.087z^2 \\ &\quad + 2.573z - 0.435. \end{aligned} \quad (23)$$

These closed-loop poles correspond to continuous time poles in the Laplace domain of  $s = [-25, -25, -40, -40, -70]$ . Implementation of a polynomial pole-placement controller requires inclusion of an observer polynomial ( $A_o$ ) with proper order to ensure the existence of a causal solution. The observer polynomial was specified to be

$$A_o(z) = A_m(z). \quad (24)$$

A minimal order causal solution is solved for the Diophantine equation

$$A(z)(z - 1)R'_1(z) + B(z)S(z) = A_o(z)A_m(z) \quad (25)$$

where

$$G'_p(z) = \frac{T_p(z)}{f_{ref}(z)} = \frac{A(z)}{B(z)} \quad (26)$$

as

$$\begin{aligned} R(z) &= (z - 1)R'_1(z) = z^5 - 4.252z^4 + 7.225z^3 \\ &\quad - 6.130z^2 + 2.598z - 0.440 \\ S(z) &= 1.393z^5 - 5.888z^4 + 9.948z^3 - 8.394z^2 \\ &\quad + 3.537z - 0.595 \\ M(z) &= 1.202z^5 - 5.089z^4 + 8.641z^3 - 7.315z^2 \\ &\quad + 3.092z - 0.522. \end{aligned} \quad (27)$$

Since  $T_{ref}$  is a constant for this torque regulation problem, the control implementation of the filter  $M$  can be replaced by its static gain  $M(1)$ . This design has a gain margin of 2.55 and a phase margin of  $60.6^\circ$ . As shown in Fig. 5, the transient response to a unit step disturbance is significantly faster than that of the previous PI design.

## VII. EXPERIMENTAL RESULTS

Representative results for the PI and pole placement control methods are given in the following sections. The pole placement controller was implemented using both the power and spindle speed based torque prediction schemes. Since the PI controller performance was deemed unacceptable using power-based torque feedback, the spindle-speed based approach was not pursued. In each experiment, machining began under constant cutting conditions of  $f_{ref} = 0.002$  ipr and  $N_{ref} = 2400$  r/min, and feedback control was initiated during phase B. In the figures that follow, the command feed (lower light trace), actual feed (lower heavy trace), torque data measured by the dynamometer (upper light trace), and the predicted

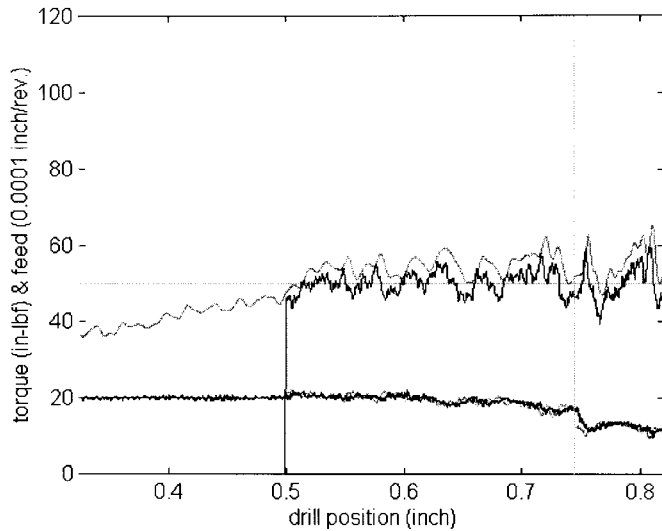


Fig. 6. Pole placement with power based torque prediction feedback (upper heavy line: feedback torque using power sensor, upper light line: dynamometer torque measurement, Lower heavy line: actual feed, Lower light line: feed command control signal).

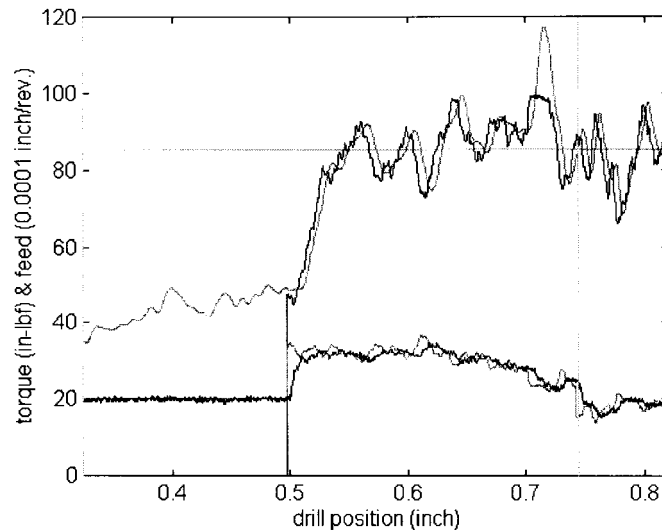


Fig. 7. Pole placement with power based torque prediction feedback (Trace legends same as Fig. 6).

torque, either by power sensor or speed sensor approach, used as feedback signal (upper heavy trace) are shown as a function of drilling depth. The plots show data collected during phase B and C, separated by a light vertical line at 0.745 inch. The set point is also shown as a horizontal line. The power sensor has a saturation limit around the equivalence of 100 in-lb for 2400 r/min spindle speed.

**Power-Based Torque Prediction:** A series of experiments were conducted for set point values from 40 to 85 in-lb. Figs. 6 and 7 show the representative experimental results of the pole placement control using the power-based torque prediction as the feedback signal for a set point of 50 and 85 in/lb, respectively. The controllers achieve tighter regulation for lower torque references. This may be attributed to the larger feed values (and hence, larger chip sizes) associated with higher references, which lead to more severe chip congestion

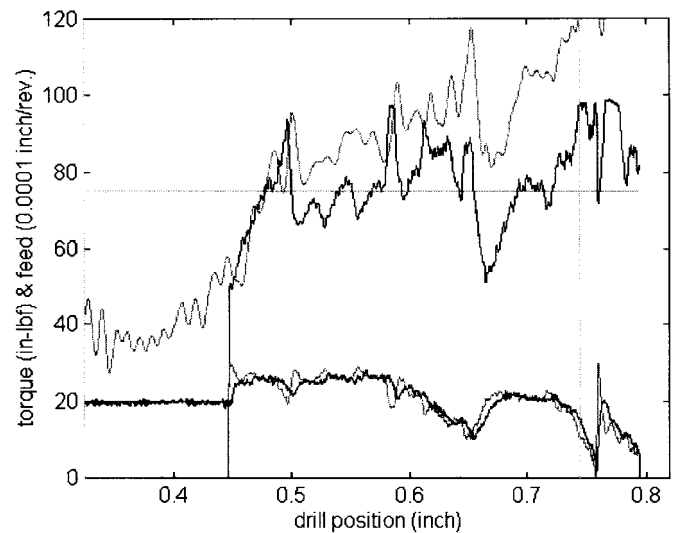


Fig. 8. Pole placement control without gain switching (trace legends same as Fig. 6).

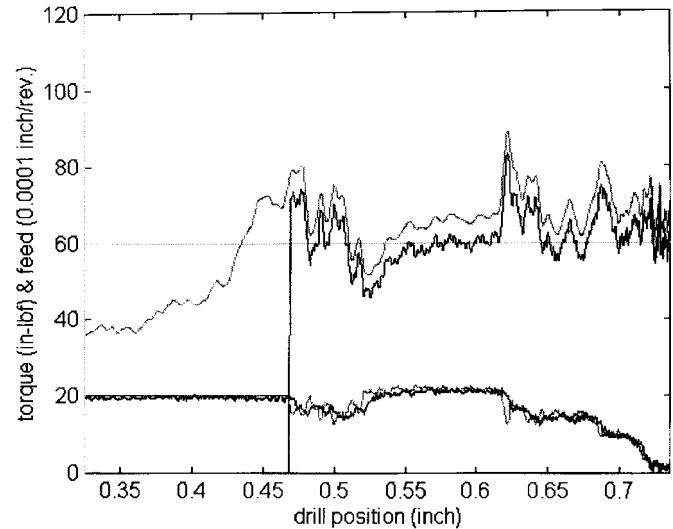


Fig. 9. Example of substantial chip congestion in closed-loop control (trace legends same as Fig. 6).

disturbances compared to the smaller feed values (and chip sizes) realized with lower torque references. Notice from the plots that the previewed gain switching in the transition from Phase B to Phase C effectively reduces the feed and maintains the closed-loop stability and torque regulation. The plots also show significant delay between the feed command and the actual feed.

The importance of the controller gain adaptation for controller performance is demonstrated in Fig. 8. In this case, the process gain was not switched upon entering Phase C; the gain for Phase B was used throughout for the torque controlled portion of the drilling cycle. As such the response during the transition from Phase B to C is sluggish and the performance in Phase C is poor.

Fig. 9 illustrates a case where substantial torque disturbances were encountered during drilling. In this example, a very low feed was required to regulate the torque reference

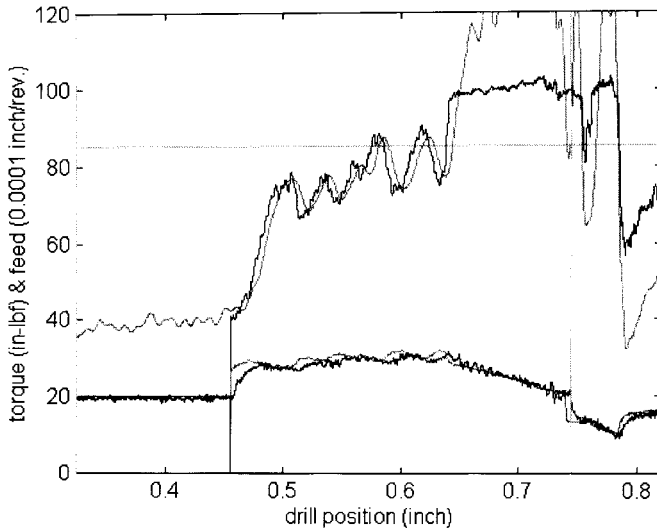


Fig. 10. PI control with power-based torque prediction feedback (trace legends same as Fig. 6).

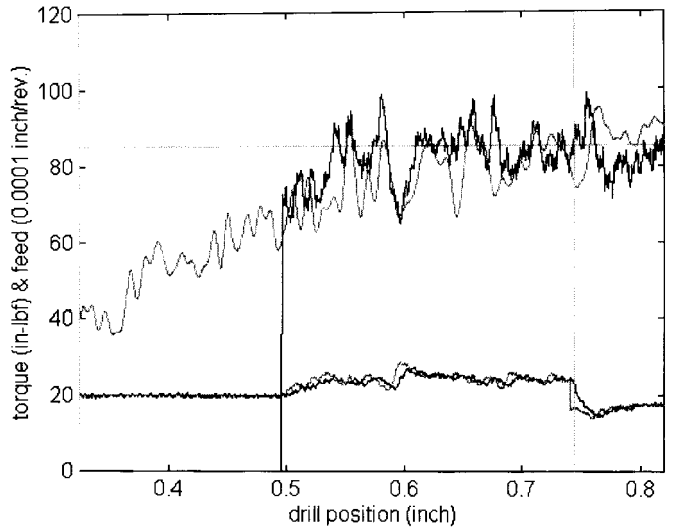


Fig. 12. Pole placement with spindle speed-based torque prediction feedback (trace legends same as Fig. 11).

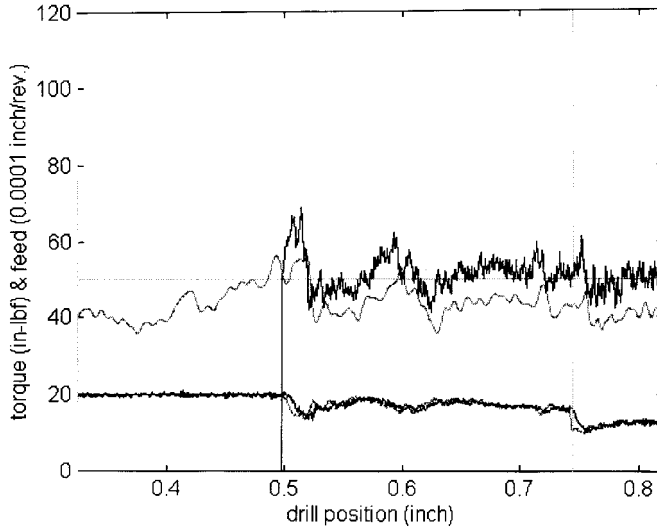


Fig. 11. Pole placement with spindle speed-based torque prediction feedback (trace legends same as Fig. 6 except that upper heavy line is the feedback torque using spindle speed-based torque prediction).

with the pole placement control. The tool was retracted to remove the jammed chips on the tool before entering Phase C to complete the cycle. It is most likely that the tool would have been catastrophically damaged had this been open-loop constant feed drilling.

As a comparison, Fig. 10 shows the result of a representative PI control performance. As expected the slow response was unable to bring the torque level down for a substantial drilling disturbance.

**Spindle-Speed Based Torque Prediction:** The pole placement controller parameters in (36) were recalculated based on the speed-based sensor model,  $G_{s,r/min}(s)$ , given by (21), included in the overall open-loop transfer function model. With respect to the overall transfer function, the difference between  $G_{s,r/min}(s)$  and  $G_{s,power}(s)$  is reflected in the total delay,  $L_{tot}$ . The remainder of the control design procedure is

identical to that described in Section VI-C, with appropriate modifications to the system model from the power-based to speed-based torque prediction model.

Representative experimental data from feedback control using spindle-speed based torque prediction is given in Figs. 11 and 12 for a torque reference of 50 and 85 in/lbs, respectively. These results demonstrate the viability of using spindle speed measurements for closed-loop torque control. The controller performance is in general similar to the power-based feedback cases except with slightly better regulation and transient response characteristics because of the shorter sensor delay.

## VIII. DISCUSSIONS AND CONCLUSIONS

A closed-loop torque controller was designed and implemented for a form tool drilling operation. This controller adequately regulated the total tool torque, and thus, avoided tool breakage. Based on the torque reference selected, this controller can also decrease the cycle time compared to open-loop, constant feed drilling. In general, higher torque references correspond to lower cycle times.

For control purposes, the drilling process feed/torque dynamic behavior was adequately modeled as a first-order, linear system with time-varying gain (due to the form tool geometry). The process gain was approximated as piece-wise constant, and varied as a function of the machining Phases corresponding to the tool geometry. The process gain was estimated off-line using experimental data. This is an important result for practical implementation, since on-line estimation of the feed-torque model is not required. It is important to note that on-line estimation of the process gain would, in general, be quite difficult due to the presence of the disturbance torque,  $T_d$ . The problem of on-line process gain estimation is clearly illustrated by the data shown in Fig. 2. Recall that these examples correspond to consecutive drilling tests under identical operating conditions. In the first hole, no significant disturbance torque occurred, while in the subsequent hole,



a large disturbance was present that led to catastrophic tool breakage.

For this study, variable gain PI and pole-placement closed-loop torque controllers were designed and implemented. The gain scheduling scheme was based on in-process position and feed velocity measurements, and also accounted for the system dead-time and dynamics. The drilling torque was predicted based on spindle speed and motor power measurements. This technique provides an inexpensive and effective method for practical controller implementation. For controller design, the sensor dynamics were modeled as a first-order system with delay. The gain scheduling scheme was adequate for both the PI and pole-placement controllers. Without process gain adaptation, significant torque overshoot occurs as drilling phase C begins, and the controller response can become quite oscillatory.

This control approach provides a technique for closed-loop process control for variable geometry form tools. In practice, conservative constant feed values are used throughout the drilling cycle to avoid tool breakage due to unpredictable process. This practice sacrifices cycle time, and may still not be effective for avoiding tool breakage (as shown in Fig. 2). Using torque control, the feed is varied as needed to regulate the cutting torque, and the production rate is maximized without tool breakage being a concern.

## REFERENCES

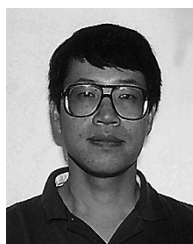
- [1] A. G. Ulsoy, Y. Koren, and F. Rasmussen, "Principal developments in the adaptive control of machine tools," *J. Dynamic Syst., Measurement, Contr.*, vol. 105, pp. 107–112, 1983.
- [2] Y. Koren and A. G. Ulsoy, "Adaptive control in machining," *Metals Handbook: Machining*, J. R. Davis, Ed., ASM Int., 9th ed., Metals Park, Ohio, vol. 16, pp. 618–626, 1989.
- [3] A. G. Ulsoy and Y. Koren, "Applications of adaptive control to machine tool process control," *IEEE Contr. Syst. Mag.*, vol. 9, no. 4, pp. 33–37, 1989.
- [4] Y. Koren and O. Masory, "Adaptive control system with process estimation," *Ann. CIRP*, vol. 30, no. 1, pp. 373–376, 1981.
- [5] O. Masory and Y. Koren, "Adaptive control system for turning," *Ann. CIRP*, vol. 29, no. 1, pp. 281–284, 1980.
- [6] O. Masory, "Real-time estimation of cutting process parameters in turning," *J. Eng. Ind.*, vol. 106, no. 3, pp. 218–221, 1984.
- [7] M. Tomizuka and S. Zhang, "Modeling and conventional/adaptive PI control of a lathe cutting process," in *Proc. 1985 Amer. Contr. Conf.*, 1985.
- [8] R. Bedini and P. C. Pinotti, "Experiments on adaptive constrained control of a CNC lathe," *J. Eng. Ind.*, vol. 104, no. 2, pp. 139–149, 1982.
- [9] L. K. Daneshmend and H. A. Pak, "Model reference adaptive control of feed force in turning," *J. Dynamic Syst., Measurement, Contr.*, vol. 108, no. 3, pp. 215–222, 1986.
- [10] L. K. Lauderbaugh and A. G. Ulsoy, "Model reference adaptive force control in milling," *J. Eng. Ind.*, vol. 111, no. 1, pp. 13–21, 1989.
- [11] M. Tomizuka, J.-H. Oh, and D. C. Dornfeld, "Model reference adaptive control of the milling process," *Control of Manufacturing Processes and Robotic Systems*, D. Hardt, Ed. New York: ASME, 1983, pp. 55–63.
- [12] M. A. Elbestawi and R. Sagherian, "Parameter adaptive control in peripheral milling," *Int. J. Machine Tools Manufacturing*, vol. 27, no. 3, pp. 399–414, 1987.
- [13] R. J. Furness, C. L. Wu, and A. G. Ulsoy, "Statistical analysis of the effects of feed, speed, and wear on hole quality in drilling," *Sensors and Signal Processing for Manufacturing*, S. Y. Liang and C. L. Wu, Eds., vol. PED-55, pp. 97–112, 1992.
- [14] R. J. Furness, A. G. Ulsoy, and C. L. Wu, "Dynamic modeling of the thrust force and torque for drilling," in *Proc. 1992 Amer. Contr. Conf.*, 1992, pp. 384–390.
- [15] ———, "Feed, speed, and torque controllers for drilling," in *Proc. 1993 Amer. Contr. Conf.*, 1993, pp. 1947–1951.
- [16] ———, "Supervisory control of drilling," in *Proc. 1993 Amer. Contr. Conf.*, 1993, pp. 1952–1958.
- [17] M. C. Shaw, *Metal Cutting Principles*. New York: Oxford Univ. Press, 1984.
- [18] C. W. de Silva, *Control Sensors and Actuators*. Englewood Cliffs, NJ: Prentice-Hall, 1989.
- [19] K. J. Astrom and B. Wittenmark, *Computer-Controlled Systems: Theory and Design*. Englewood Cliffs, NJ: Prentice-Hall, 1990.



**Richard J. Furness** received the B.S., M.S., and Ph.D. degrees in mechanical engineering from the University of Michigan, Ann Arbor, in 1987, 1988, and 1992, respectively.

He is currently a Technical Specialist in the Manufacturing Systems Department of the Ford Research Laboratory, and is the Project Leader for the Manufacturing Mechatronics and Controls group. His research interests include dynamic modeling and control of machining processes, machining system analysis and design, digital control and signal processing, intelligent sensor-based manufacturing, and open-architecture systems for machining and manufacturing process control.

Dr. Furness is a member of the American Society of Mechanical Engineers, the Society of Manufacturing Engineers, and the North American Manufacturing Research Institution of SME.



**Tsu-Chin Tsao** (S'86–M'88) received the B.S. degree from National Taiwan University in 1981, and the M.S. and Ph.D. degrees from the University of California, Berkeley, in 1984 and 1988, respectively.

He is currently an Associate Professor at University of Illinois at Urbana-Champaign (UIUC). His research interests include dynamic modeling and control of mechanical systems, manufacturing processes, and automotive systems.

Dr. Tsao is a Member of ASME and a Senior Member of SME. His research was recognized by the 1994 Best Paper Award of ASME Journal of Dynamic Systems, Measurement, and Control, UIUC College of Engineering Xerox Award for Faculty Research (1996), and ASME Dynamic Systems and Control Outstanding Young Investigator Award (1997).

**James S. Rankin II** received the B.E. degree in electrical technology from RETS Technical University in 1974.

He is currently working in the Manufacturing Systems Department at the Ford Research Laboratory. He is the author or coauthor of numerous publications and has received several patents for his work over the past 20 years with Ford.

**Michael J. Muth** received the B.S.E.E. degree from Valparaiso Technical Institute, Valparaiso, IN, in 1974.

He is a principal computer applications engineer with Ford Research Laboratory and has worked for the Ford Motor Company for over 26 years in various research positions specializing in real-time data acquisition and control.

**Kenneth W. Manes** received a Bachelor of Science degree in Manufacturing Engineering Technology from Wayne State University, Detroit, MI.

He is a Manufacturing Engineer in Starter Motor Operations in the Visteon Powertrain Control Systems Division. He is a Senior Member of the Society of Manufacturing Engineers.